International Journal for Parasitology: Drugs and Drug Resistance 21 (2023) 74–80

Contents lists available at ScienceDirect

International Journal for Parasitology: Drugs and Drug Resistance

journal homepage: www.elsevier.com/locate/ijpddr

Effect of the pseudomonas metabolites HQNO on the *Toxoplasma gondii* RH strain *in vitro* and *in vivo*

Jiao Mo [a,1], Hongfei Si [c,1], Siyang Liu [a], Qingyuan Zeng [a], Minghao Cai [a], Zhendi Liu [a], Jiyu Zhang [d], Jingjing Fang [b], Jili Zhang [a,b,d,*]

[a] School of Medicine, Ningbo University, Ningbo, China
[b] Intensive Care Unit, The Affiliated Hospital of Medical School, Ningbo University, Ningbo, China
[c] College of Pharmacy, Jinan University, Guangzhou, China
[d] Lanzhou Institute of Husbandry and Pharmaceutical Sciences, Chinese Academy of Agricultural Science, China

ARTICLE INFO

Keywords:
HQNO
Toxoplasma gondii
Invasion
Proliferation
Pharmacokinetics
In vivo
TEM

ABSTRACT

Toxoplasmosis is a widespread disease in humans and animals. Currently, toxoplasmosis chemotherapy options are limited due to severe side effects. There is an urgent need to develop new drugs with better efficacy and few side effects. HQNO, a cytochrome *bc*1 and type II NADH inhibitor in eukaryotes and bacteria, possesses extensive bioactivity. In this study, the cytotoxicity of HQNO was evaluated in Vero cells. The *in vitro* effects of HQNO were determined by plaque assay and qPCR assay. To determine the *in vivo* effect of HQNO, pharmacokinetic experiments and *in vivo* infection assays were performed in mice. The changes in tachyzoites after HQNO exposure were examined by transmission electron microscopy (TEM), MitoTracker Red CMXRos staining, ROS detection and ATP detection. HQNO inhibited *T. gondii* invasion and proliferation with an EC_{50} of 0.995 μM. Pharmacokinetic experiments showed that the C_{max} of HQNO (20 mg/kg·bw) was 3560 ± 1601 ng/mL (13.73 μM) in healthy BALB/c mouse plasma with no toxicity *in vivo*. Moreover, HQNO induced a significant decrease in the parasite burden load of *T. gondii* in mouse peritoneum. TEM revealed alterations in the mitochondria of *T. gondii*. Further assays verified that HQNO also decreased the mitochondrial membrane potential (ΔΨm) and ATP levels and enhanced the level of reactive oxygen species (ROS) in *T. gondii*. Hence, HQNO exerted *anti-T. gondii* activity, which may be related to the damage to the mitochondrial electron transport chain (ETC).

1. Introduction

Toxoplasma gondii (T. gondii) is an intracellular parasite that can widely infect humans and other warm-blooded animals and causes zoonosis. It is estimated that approximately 30–50% of the world's population has been infected with *T. gondii* (Robert-Gangneux and Dardé, 2012). Furthermore, toxoplasmosis results in ocular infection in 10% of immunocompetent people in South America (Gómez et al., 2018). In immunodeficient patients, such as AIDS patients and pregnant women, *T. gondii* infection often leads to serious central nervous system diseases, teratology, and even death (Robert-Gangneux and Dardé, 2012; Bergin et al., 1992). The combination of pyrimidine and sulfadiazine is the gold-standard therapy (Deng et al., 2019). However, this therapy needs to be improved due to the significant bone marrow toxicity and ineffectiveness against chronic infection cysts of *T. gondii* (Giovati et al., 2018). Thus, exploiting novel therapeutic drugs is essential for future intervention strategies (Konstantinovic et al., 2019).

The mitochondrial electron transport chain (ETC) is an important

Abbreviations: Transmission electron microscopy, (TEM); Mitochondrial membrane potential, (ΔΨm); Reactive oxygen species, (ROS); Electron transport chain, (ETC); *Toxoplasma gondii*, (*T. gondii*); Type-II NADH dehydrogenases, (NDH-2); Endochin-like quinolone, (ELQ); 2-Heptyl-4-hydroxyquinoline N-oxide, (HQNO); Charge transfer complex, (CTC); Mitochondrial membrane permeability transition pore, (mPTP); Dissolved in dimethyl sulfoxide, (DMSO); Dulbecco's modified Eagle's medium, (DMEM); Foetal bovine serum, (FBS); Nonessential amino acids, (NEAAs); Parasitophorous vacuoles, (PVs); 50% effective concentration, (EC_{50}); Standard deviation, (SD); Akaike Information Criterion, (AIC); Peak plasma concentration, (C_{max}); Area under the plasma curve, (AUC); Half-life, ($T_{1/2}$); Peak time, (T_{max}); Adenosine triphosphate, (ATP); hydroxy-2-dodecyl-4(1H) quinolone, (HDQ); Half-maximal inhibitory concentration, (IC_{50}).

* Corresponding author. School of Medicine, Ningbo University, Ningbo, Zhejiang, 315211, China.
E-mail address: zhangjili@nbu.edu.cn (J. Zhang).

[1] The authors contributed equally to this work.

https://doi.org/10.1016/j.ijpddr.2023.02.001
Received 22 October 2022; Received in revised form 31 January 2023; Accepted 1 February 2023
Available online 4 February 2023

target for the development of anti-parasitic drugs due to several crucial biological functions, such as maintaining the mitochondrial membrane potential (ΔΨm) and generating ATP through oxidative phosphorylation. Therefore, it is indispensable for the survival of many intracellular apicomplexans, including *T. gondii* (Acharjee et al., 2021). In particular, *T. gondii* has only one linked inner mitochondrial membrane (Melo et al., 2000). Furthermore, *T. gondii* lacks complex I of the mitochondrial respiratory chain and contains rotenone-insensitive, nonproton pumping type-II NADH dehydrogenases (NDH-2), which are not "alternative" in the human host, indicating that NDH-2 might be a prospective therapeutic target for *T. gondii* (Melo et al., 2004; Lin et al., 2008; Kerscher et al., 2008). Additionally, electrons are transported through complexes III (cytochrome *bc*1 complex) and IV in the ETC, coupled with proton translocation through the inner mitochondrial membrane, generating a proton gradient that ATP synthase uses to synthesize ATP (Musso et al., 2020). The Qo and Qi sites of cytochrome *bc*1 are targets of a variety of antiparasitic drugs, such as atovaquone and endochin-like quinolone (ELQ). A dual inhibitor of complex III can alleviate drug resistance and achieve an excellent therapeutic effect (Smith et al., 2021). Accordingly, drugs that target NDH-2 and cytochrome *bc*1 would be effective against *T. gondii*.

2-Heptyl-4-hydroxyquinoline N-oxide (HQNO), a metabolite from *P. aeruginosa*, exerts antibacterial activity through high-affinity binding of type II NADH quinone oxidoreductase, which is involved in the respiratory chains of bacteria, including gram-positive bacteria (Thierbach et al., 2017; Radlinski et al., 2017; Sena et al., 2015). HQNO can be embedded in the Q-site of NDH-2, in which the quinone-head group is clamped by Q317 and I379 residues and hydrogen bonds to FAD. HQNO can block quinone substrates from entering FAD and interfere with ATP synthesis through competitive or non-competitive inhibition (Petri et al., 2018). In particular, the charge transfer complex (CTC), generated from the electron transfer process, could change the conformation of HQNO and the quinone binding pocket, which is conducive to the binding of HQNO to NDH-2 but not for the binding of HQNO to quinone (Sena et al., 2018). HQNO has also been proven to be an inhibitor, binding to the Qi site of cytochrome *bc*1 in eukaryotes and bacteria. When the Qi site is blocked, semiquinone radicals can react with O_2 to produce superoxide, a reactive oxygen species (ROS). The increase in ROS in organisms results in an imbalance in mitochondrial membrane potential and opening of the mitochondrial membrane permeability transition pore (mPTP), thus leading to mitochondrial dysfunction and secretion of its contents and finally apoptosis (Hazan et al., 2016; Wu and Seyedsayamdost, 2017; Thierbach et al., 2019). Consequently, HQNO has devastating effects on energy production pathways in multiple species by interfering with NDH-2 and cytochrome *bc*1 in the ETC. HQNO may be a potential compound against *T. gondii*. In this study, we explored the activity of HQNO against the *T. gondii* RH strain *in vitro* and *in vivo* and its mechanism of action.

2. Materials and methods

2.1. Drugs, tachyzoites and cell culture

HQNO (HY-130055, 99.14%) was purchased from Med Chem Express (MCE, USA) and dissolved in dimethyl sulfoxide (DMSO, Sigma, USA) to prepare a stock solution of 10 mM.

The tachyzoites of the *T. gondii* RH strain used in this study were inoculated in Vero cells in Dulbecco's modified Eagle's medium (DMEM) supplemented with 1% foetal bovine serum (FBS), which was generously donated by the Lanzhou Institute of Husbandry and Pharmaceutical Sciences, China. The tachyzoites were collected and counted as described previously (Sepúlveda-Arias and Juan, 2014).

Vero cells were cultured in DMEM with 10% FBS, streptomycin (100 μg/mL), 1% nonessential amino acids (NEAAs), penicillin (100 U/mL) and 1% GlutaMAX at 37 °C in an atmosphere containing 5% CO_2.

2.2. Cytotoxicity assay

Vero cells were seeded in 96-well plates at 1×10^4 cells/well, cultured to obtain a monolayer, and subjected to HQNO at final concentrations of 0.78125, 1.5625, 3.125, 6.25, 12.5, 25, 50 or 100 μM in DMEM with 1% FBS. Cells were incubated in DMEM without compound as a control. After 24 h, Vero cells were incubated with CCK-8 solution (Biomake, USA) for 1 h, and the absorbance was detected at 450 nm with a Multiskan GO instrument (Thermo Fisher Scientific, MA, USA). Cell survival rate (%) = (absorbance of drug treatment group - absorbance of the blank control group)/(absorbance of control group - absorbance of the blank control group) × 100%. The concentration range of HQNO without Vero cytotoxicity was used in the following *in vitro* activity experiments. Triplicate independent experiments were performed.

2.3. Plaque assay

Plaques were used to evaluate the activity of HQNO on *T. gondii* proliferation and invasion in host cells. For the anti-proliferation assay, Vero cell monolayers were infected with *T. gondii* tachyzoites (2×10^4 cells/well) for 8 h, and then, DMEM containing HQNO (0.625, 1.25, 2.50, 5.00 or 10.0 μM) with 1% FBS was added for 24 h incubation. For the anti-invasion assay, *T. gondii* tachyzoites (2×10^4 cells/well) were incubated with DMEM containing HQNO (0.625, 1.25, 2.50, 5 or 10.0 μM) and then used to infect Vero cells for 2 h. DMEM without drug was used in the control groups. After 48 h, 72 h, and 96 h of culture, the plaques were washed three times with PBS, and 4% fixative solution (paraformaldehyde) was used to fix the plaques. Samples were stained with crystal violet for 10 min and then washed three times in PBS. After drying at room temperature, the number of parasitophorous vacuoles (PVs) in each field and the number of parasites in each PV were observed by electron microscopy, and at least 20 random fields per well were counted under a 40 × objective lens.

2.4. Anti-invasion assessment of HQNO

Vero cell monolayers were incubated with DMEM containing 1% FBS and 0.625, 1.25, 2.50, 5.00 or 10.0 μM HQNO, 11.5 μM azithromycin as a positive control or no drug as a negative control. Then, 2×10^6 fresh parasites per well were added, and after 2 h, the cells were washed twice with DPBS and then incubated with DMEM for 24 h. The sample DNA was extracted with DNAiso reagent, and the 529 bp repeat unit of *T. gondii* was detected by qPCR. The primers and amplification conditions used were described in a previous study (Zhang et al., 2019a, Mital and Ward, 2008). Triplicate independent experiments were performed.

2.5. Anti-proliferation activity of HQNO

Vero cells were cultured to monolayers in 6-well plates and then infected with 2×10^5 tachyzoites per well. After 8 h, various concentrations of HQNO (0.625, 1.25, 2.50, 5.00, or 10.0 μM) and azithromycin as a positive control were added to 6-well plates. DMEM containing 1% FBS without drug was added as a negative control for 24 h. The total DNA of the cell samples was extracted with DNAiso reagent, and the *T. gondii* 529 bp repeat unit was detected by qPCR (Zhang et al., 2019a). The 50% effective concentration (EC_{50}) and therapeutic index of HQNO against *T. gondii* were calculated. The results represent the mean ± standard deviation (SD) of at least three independent experiments.

2.6. Safety assay of HQNO in mice

HQNO was dissolved in saline with 10% ethanol and 10% Cremophor EL to a concentration of 2 mg/mL for intraperitoneal injection. BALB/c mice were treated with 5, 10, or 20 mg/kg HQNO, solvent without drug or PBS (as a control) once a day for 7 days and observed for an additional 23 days. During this period, the clinical toxicity of various

drug doses was observed.

2.7. The pharmacokinetics of HQNO in mouse plasma

HQNO was dissolved in saline with 10% ethanol and 10% Cremophor EL at a concentration of 2 mg/mL to prepare a stock solution. The prepared HQNO was intraperitoneally injected into 9 BALB/c female mice at a dose of 20 mg/kg based on the results of a safety assay. Blood samples (100 μL) were collected at 0 h, 0.083 h, 0.25 h, 0.5 h, 1 h, 2 h, 4 h, 8 h, 12 h and 24 h. After all blood samples were centrifuged at 3000 rpm for 10 min, plasma samples were collected and immediately stored at −20 °C until analysis.

The pharmacokinetic parameters were calculated using WinNonlin professional software version 8.0 (Pharsight, Mountain View, California, USA). The optimal pharmacokinetic model was determined according to the minimum Akaike Information Criterion (AIC) value and used for data fitting and parameter estimation. The peak plasma concentration (C_{max}), area under the plasma curve (AUC), half-life ($T_{1/2}$) and peak time (T_{max}) were expressed as the mean ± SD (Zeng et al., 2022).

2.8. The in vivo activity of HQNO against T. gondii

Each BALB/c mouse was intraperitoneally injected with 1×10^3 *T. gondii* tachyzoites for 4 h and then treated with HQNO (20 mg/kg·bw), the positive control drug (50 mg/kg·bw azithromycin) or PBS (negative control). For all groups, the treatment was administered by intraperitoneal injection once a day for 7 consecutive days. One millilitre of ascites was aspirated, washed three times, and centrifuged to extract DNA of *T. gondii*, and the number of parasites in each sample was detected by RT−PCR, as previously described (Zhang et al., 2019b). The number of tachyzoites in a sample was calculated from a standard curve ($Y = -3.673x + 34.341$; $R^2 = 0.9997$) constructed with serially diluted (3.00×10^6 to 3.00×10^3/mL) DNA samples from RH strain tachyzoites.

2.9. Transmission electron microscopy (TEM) analysis

To observe the internal structure of parasites with TEM, Vero cells were first seeded in T25 flasks and then treated with 2×10^6 *T. gondii* tachyzoites for 8 h. After adding 5 μM HQNO, the cells were cultured for 8 or 24 h. The cells were digested with TrypLE Express for 2 min, washed twice with PBS, and fixed with 2.5% glutaraldehyde at 4 °C for 12 h. Glutaraldehyde was removed with PBS, and the cells were fixed with 1% osmium acid solution in the dark for 1.5 h. The samples were then washed with PBS, dehydrated in a series of alcohol concentrations, dehydrated with acetone, and embedded in Epon. Finally, ultrathin sections were stained with uranyl acetate and lead citrate and observed under TEM (Tecnai Spirit Bio-TWIN, Thermo, FEI, USA) (Zhang et al., 2019b).

2.10. Mitochondrial membrane potential in T. gondii tachyzoites

T. gondii tachyzoites in Vero cell monolayers were incubated with DMEM with 1 or 5 μM HQNO for 8 or 24 h, washed with PBS, and coincubated with the MitoTracker Red CMXRos probe (50 nM, C1049B, Beyotime Biotechnology, China) for 20 min. The fluorescence intensity of the samples was observed by a multifunctional microplate reader (Zhang et al., 2021).

2.11. Adenosine triphosphate (ATP) level in T. gondii tachyzoites

T. gondii tachyzoites infecting Vero cells were incubated with DMEM with 1 or 5 μM HQNO for 8 or 24 h. Then, fresh *T. gondii* tachyzoites were isolated, purified, and lysed, and the ATP levels were detected; the results are expressed in μmol/L (μM). Three independent experiments were repeated for evaluation (Zhang et al., 2019a).

2.12. ROS production assay

T. gondii tachyzoites infecting Vero cells were treated with DMEM with HQNO (1 or 5 μM) or without HQNO as a control. Then, 2×10^6 *T. gondii* tachyzoites were isolated from the Vero cells and seeded in black 96-well microplates in DMEM, washed with PBS twice, and then coincubated with 7.5 μM CMH2DCFDA (Solarbio, D6470) for 10 min. After incubation, to remove the excess probe, *T. gondii* tachyzoites were washed three times with PBS. *T. gondii* tachyzoites were resuspended in 100 μL/well PBS, and their fluorescence intensity was measured by a Tecan Infinites M200 microplate reader with excitation and emission filters set at 488 nm and 525 nm, respectively (Sul and Ra, 2021).

2.13. Statistical analysis of the data

Data were analyzed by SPSS 23.0 (SPSS, Inc.; Chicago, IL, USA) and GraphPad Prism 6 (San Diego, CA) software. Data are presented as the mean ± SD. Student's t-test was used for the comparison of group means, and $P \leq 0.05$ was considered significant.

3. Results

3.1. Cytotoxicity activity

The cytotoxicity of HQNO was evaluated in the Vero cell line (Fig. 1). The results showed that HQNO inhibited cell growth in a dose-dependent manner, with a half inhibitory concentration of 33.38 μM. The concentration of DMSO used in the experiment was less than 1% (v/v), which is not toxic to the cells. The cytotoxicity assay provides a safe dose range for subsequent tests.

3.2. Plaques formed by T. gondii-infected cells

Plaques of *T. gondii*-infected Vero cells were formed. Fig. 2 shows that HQNO significantly reduced the invasion and proliferation ability of *T. gondii* after 48 h, 72 h, and 96 h of incubation ($P \leq 0.05$). Specifically, compared with the control groups, the PV number decreased significantly (Fig. 2a–b, $P \leq 0.05$), both pre-and post-infection, and the average number of tachyzoites within the PVs was also decreased (Fig. 2c–h, $P \leq 0.05$). By comparison, the plaques formed still showed dose-dependent inhibition of tachyzoite growth in the range of 0.625–10 μM after 6 days of incubation, as shown in Fig. 3a–d.

3.3. HQNO inhibited T. gondii tachyzoite proliferation and invasion

The ability of HQNO to inhibit the intracellular proliferation of

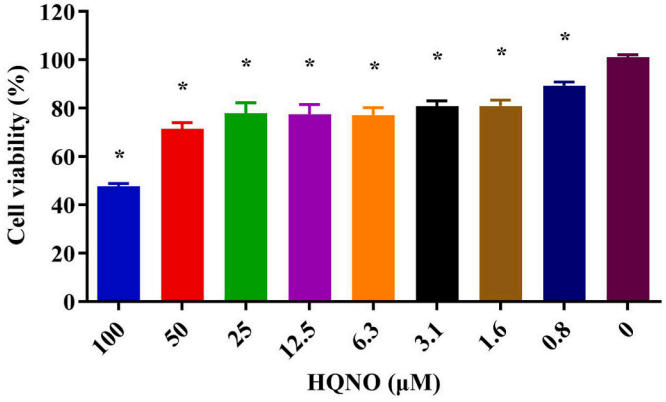

Fig. 1. The cytotoxicity of HQNO on Vero cells. All data are presented as the mean ± standard deviation (SD) from 3 replicate experiments. *$P \leq 0.05$ compared with the control.

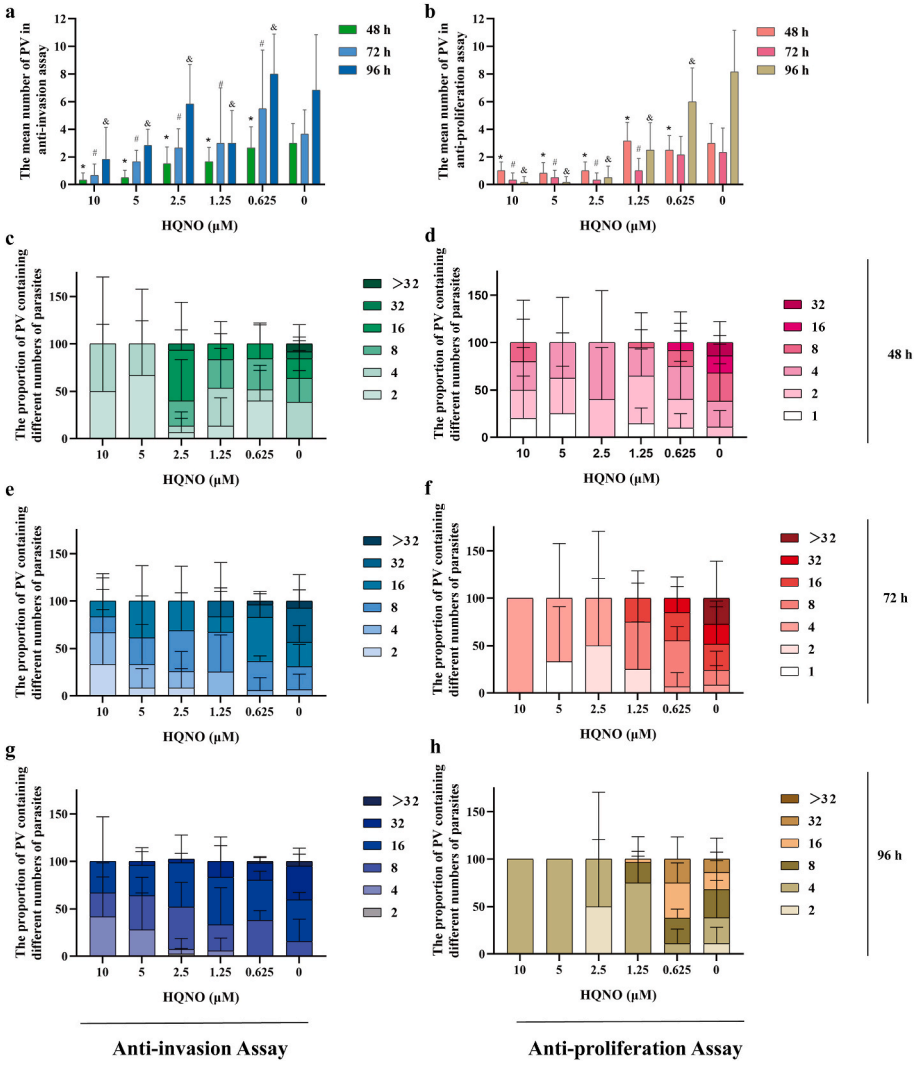

Fig. 2. Plaques formed by *T. gondii* infected cells. HQNO decreased the number of PV and parasite number in PV of *T. gondii* both in invasion and proliferation after 48 h, 72 h, 96 h incubation, as shown in Fig. 2a–h. $^{*}P \leq 0.05$ compared with the control for 48 h $^{\#}P \leq 0.05$ compared with the control for 72 h $^{\&}P \leq 0.05$ compared with the control for 96 h.

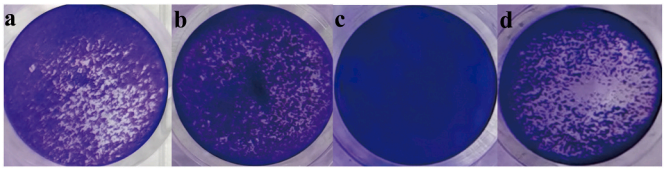

Fig. 3. Plaques formed is dose-dependent inhibition of tachyzoites growth after 6 days of incubation. 0.625 μM treatment group (Fig. 3a), 2.5 μM treatment group (Fig. 3b), 10 μM treatment group (Fig. 3c). The Vero cells were not treated as control (Fig. 3d).

T. gondii tachyzoites was determined by qPCR. HQNO significantly ($P \leq 0.05$) inhibited *T. gondii* tachyzoite intracellular proliferation compared with the control group in a concentration-dependent manner in the range of 0.625–10 μM (Fig. 4b). The EC_{50} of HQNO for *T. gondii* tachyzoite growth inhibition was 0.995 μM, and the therapeutic index was 33.55. The inhibition rate of azithromycin, a positive control drug, on the intracellular proliferation of *T. gondii* tachyzoites was 37.50%.

In the anti-invasion assay, compared to controls, HQNO in the 0.625–10 μM range significantly inhibited *T. gondii* invasion ($P \leq 0.05$) (Fig. 4a). The anti-invasion inhibition rate in the positive control group

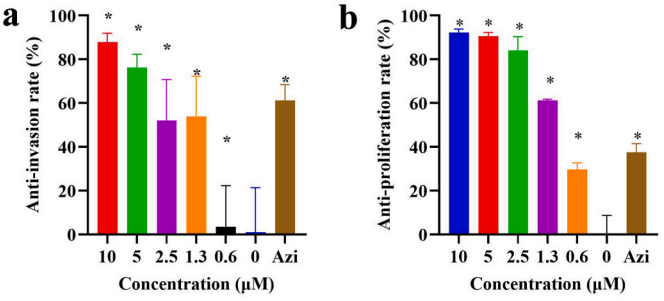

Fig. 4. The *anti-T. gondii* invasion activity of HQNO (a). The anti-proliferation effect of HQNO on *T. gondii* infected Vero cells was examined with qPCR (b). The inhibition rate of tachyzoite proliferation or invasion in the experimental group was compared with that in the control group. Data are presented as mean ± SD of three independent experiments. $^{*}P \leq 0.05$ compared with the control group.

was 53.98%.

3.4. The anti-T. gondii activity of HQNO in vivo

To determine the HQNO dose safety *in vivo*, mice were intraperitoneally injected with HQNO (5, 10 or 20 mg/kg) over 7 days, during which no obvious clinical toxicity was observed. The plasma concentration of HQNO was measured after mice were injected intraperitoneally at a dose of 20 mg/kg. The main pharmacokinetic parameters are listed in Table 1. The C_{max} of HQNO in mice was 3560 ± 1601 ng/mL (13.727 μM), T_{max} was 0.083 ± 0.000 h, $AUC_{0\text{-}t}$ was 3864 ± 301 h/ng·mL, and $MRT_{0\text{-}t}$ was 1.560 ± 0.446 h. The mean plasma concentration-time profile after intraperitoneal injection of HQNO into mice is shown in Fig. 5a. At the same dose, HQNO was used to treat mice infected with *T. gondii*. After treatment for 7 days, the results indicated that HQNO significantly decreased the parasite burden in mouse peritoneum ($P \leq 0.05$) (Fig. 5b).

3.5. Ultrastructural changes in T. gondii after HQNO treatment

Ultrastructural changes in tachyzoites were observed by TEM. In the control group, *T. gondii* tachyzoites proliferated in the form of binary fission and formed parasitophorous vacuoles (PVs) surrounded by host cell mitochondria. Parasite proliferation in PVs resulted in aggregation into banana-like morphology after 24 h, and the organelles, including nuclei, mitochondria, rhoptries, dense granules and a conoid, were clearly visible (Fig. 6a–b). After incubation with HQNO (5 μM) for 8 h, the interior of the parasite contained numerous vacuoles with disorganized organelle arrangement and various degrees of deformation. In particular, the mitochondria were swollen, the inner ridge structure had been lost, and the membrane was intact (Fig. 6c). After 24 h of treatment, HQNO (5 μM) induced distortion or even rupture of the PV membrane, completely disordered internal organelles and barely distinguishable mitochondrial morphology, and parasite death (Fig. 6d). HQNO does not affect the mitochondria of host cells around PVs. The distinct changes indicated that the mitochondrion may be a targeted organelle of HQNO against *T. gondii*.

3.6. The effect of HQNO on mitochondria of T. gondii tachyzoites

To further explore the mechanism of HQNO against *T. gondii*, the ΔΨm, ATP and ROS levels were measured. Eight or 24 h of treatment with HQNO induced significant dose-dependent decreases in both the ΔΨm and ATP levels in cellular parasites compared with those in the control group ($P \leq 0.05$; Fig. 7a and c), which were relevant to mitochondrial oxidative phosphorylation. Compared with that in the control group, HQNO induced an increase in ROS levels in *T. gondii* in a dose-dependent manner, as shown in Fig. 7b.

4. Discussion

Toxoplasmosis chemotherapy is often accompanied by serious toxic and severe side effects, and there is an urgent need to develop novel drugs with high efficiency and low toxicity against *T. gondii* tachyzoites or bradyzoites (Konstantinovic et al., 2019; Acharjee et al., 2021). Given the important role that mitochondrial function plays in the *T. gondii* life cycle, the ETC has been a promising drug target for the development of *anti-T. gondii* drugs. HQNO, a quinolone compound that is a methylated derivative of *Pseudomonas* metabolites, is the most potent inhibitor of NDH-2 and cytochrome *bc*1 in many species, including *Gluconobacter oxydans*, *Yarrowia lipolytica*, *S. cerevisiae*, and *S. aureus* (Petri et al., 2018; Thierbach et al., 2017). This study discussed the *anti-T. gondii* activity of HQNO *in vitro* and in an infected mouse model and explored its mechanism of action.

In this study, HQNO exerted potent anti-*T. gondii* activity without obvious cytotoxic effects on Vero cells. HQNO significantly reduced the number of PVs and the average number of tachyzoites within the PVs. It inhibited intracellular replication and invasion in the range of 0.625–10 μM, and the EC_{50} of HQNO was 0.995 μM. In particular, the therapeutic index of HQNO on *T. gondii* was 33.55, which indicated that HQNO has a wide safety range. *In vivo*, mice treated with 20 mg/kg·bw HQNO had no obvious toxic side effects. After this dose of HQNO was injected intraperitoneally, we evaluated the pharmacokinetics of HQNO in mouse plasma, and the results indicated that the C_{max} (13.727 μM) was higher than the EC_{50} in mice, which may help HQNO exert its anti-*T. gondii* activity *in vivo*. To explore the *in vivo* effect of HQNO, a mouse model

Table 1
Main pharmacokinetic parameters of HQNO after intraperitoneal administration.

Parameters (Units)	Mean ± SD
Kel (h^{-1})	0.485 ± 0.190
$T_{1/2}$ (h)	1.430 ± 0.393
T_{max} (h)	0.083 ± 0.000
C_{max} (ng/mL)	3560 ± 1601
$AUC_{0\text{-}t}$ (h/ng·mL)	3864 ± 301
$AUC_{0\text{-}inf}$ (h/ng·mL)	3883 ± 308
$MRT_{0\text{-}t}$ (h)	1.560 ± 0.446
$MRT_{0\text{-}inf}$ (h)	1.624 ± 0.464

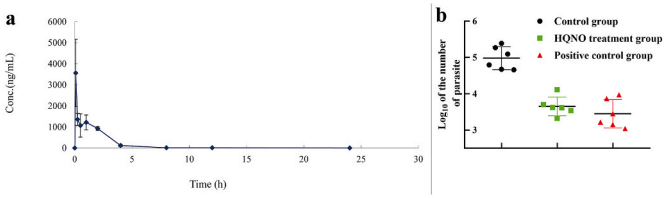

Fig. 5. Mean plasma concentration-time profile intraperitoneal injection of HQNO to mice (n = 3) (Fig. 5a). Administration of HQNO decreased the *T. gondii* load in acute infected mice (Fig. 5b).

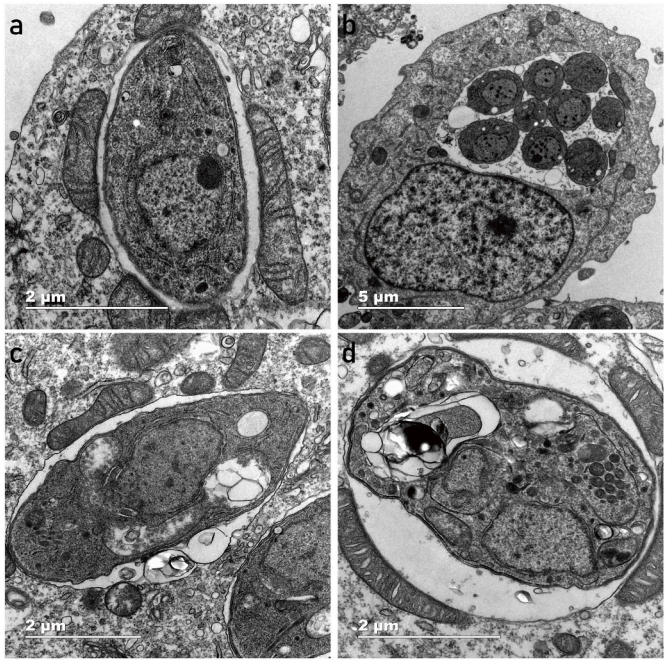

Fig. 6. Ultrastructural changes in *T. gondii* infected Vero cells after HQNO (5 μM) treatment or not. *T. gondii* in the control group exhibited the typical morphology within the PV in (a) and (b). 8 or 24 h of treatment with HQNO induced changes in shape and structure of tachyzoites, as shown in (c) and (d). Scale bars: 2 μm (a, c, d); 5 μm (b).

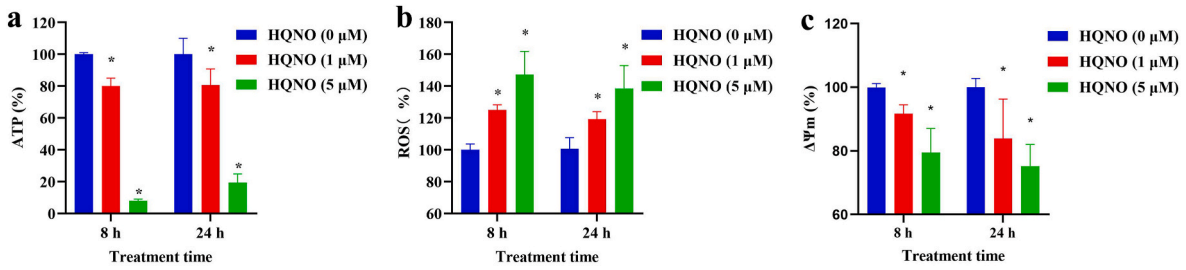

Fig. 7. HQNO induced a decrease in the ATP concentration of parasites (a) and mitochondrial membrane potential (c). HQNO induced an increase in the ROS concentration (b). Data are presented as the mean value ± SD of triplicate experiments. *$P \leq 0.05$ compared with the control group.

was established by infecting mice with the virulent RH strain of *T. gondii*. Mice were intraperitoneally injected with HQNO at a dose of 20 mg/kg or above for 7 days. During this period, HQNO significantly reduced the parasite burden in mouse ascites. A previous report indicated that the quinolone drug 1-hydroxy-2-dodecyl-4(1H) quinolone (HDQ) inhibited NDH-2 activity in a dose-dependent manner *in vitro* to exert its anti-*T. gondii* activity with a half-maximal inhibitory concentration (IC_{50}) of approximately 300 nM (Lin et al., 2008; Bajohr et al., 2010). It must be noted that the inhibition of *T. gondii* activity by HDQ was recovered after treatment. The possibility of HDQ having adverse effects on targets unrelated to the alternative NADH dehydrogenases cannot be ruled out at concentrations >2000 times greater than the IC_{50} (Saleh et al., 2007). Previous studies detected that oral treatment with ELQ-334 also reduced the parasite load of brain cysts, but the parasites could not be completely cleared (Doggett et al., 2020), and the ELQs had physical properties of low aqueous solubility and high crystallinity, which limited their oral bioavailability (Doggett et al., 2012). By comparison, HQNO exhibited potent anti-*T. gondii* activity *in vitro* and *in vivo*, and its inhibitory effect on *T. gondii* was not reversed after treatment.

To explore the mechanism of action of HQNO on *T. gondii*, TEM was used to observe the ultrastructure of parasites treated with HQNO. Herein, TEM analysis showed that HQNO (5 μM) induced mitochondrial damage and the appearance of an autophagic double membrane structure in the cytoplasm, which is a marker of apoptosis. Previous studies revealed that HQNO is a high-affinity inhibitor of NDH-2, which is vital in the respiratory chain (Thierbach et al., 2017). Its mechanism of action is interference with the ubiquinol binding site on the enzyme by competitive or noncompetitive inhibition to inhibit the energy supply of cells (Sena et al., 2018). Additionally, HQNO also leads to specific self-poisoning by disrupting the electron transduction of the cytochrome *bc*1 complex in the respiratory chain, resulting in the direct transfer of electrons that should be transferred from cytochrome C to O_2 (Hazan et al., 2016). The subsequent large production of ROS reduces the mitochondrial membrane potential and destroys the integrity of the plasma membrane, inducing bacterial cell autolysis and DNA release (Vallières et al., 2012; Hazan et al., 2016). Our experimental results also indicated that HQNO treatment indeed induced dose-dependent decreases in the ΔΨm and ATP levels in *T. gondii* and increased the ROS level, confirming that HQNO incubation affected the redox respiratory chain of *T. gondii*. In addition to the HDQ mentioned above, the quinolone drug ELQ could inhibit cytochrome *bc*1 activity by interfering with the ETC of mitochondria (Hegewald et al., 2013; Doggett et al., 2012). As HQNO was found to target both the bc1 complex and NDH-2, HQNO may have a dual mode of action on *T. gondii*. The specific mechanism of action of HQNO against *T. gondii* needs to be further explored.

5. Conclusion

In conclusion, this study proved that HQNO exerted *anti-T. gondii* activity by inhibiting the replication and invasion of *T. gondii in vitro* without cytotoxicity. HQNO also reduced the parasite burden in infected mouse tissues. The main observation by TEM of distortion of mitochondria and the decreased levels of ΔΨm and ATP and increased levels of ROS suggested that HQNO interferes with *T. gondii* mitochondrial oxidative phosphorylation. The mechanism of action of HQNO on *T. gondii* is possibly targeting NDH-2 and cytochrome *bc*1 in *T. gondii* mitochondria. Therefore, our work showed that HQNO has the potential to be developed into a novel *anti-T. gondii* drug. It is necessary to further investigate the efficacy of HQNO on different *Toxoplasma* strains and explore its specific mechanism of action.

Ethics approval and consent to participate

The study was conducted in accordance with the ARRIVE guidelines. Thirty BALB/c mice were used in this study, which was conducted by Dr. Jili Zhang at Lanzhou Institute of Husbandry and Pharmaceutical Sciences, Gansu Province, China from April to May 2020. All experimental methods, the animal care and the environment of the barn strictly comply with the guidelines for the Care and Use of Laboratory Animals, Lanzhou Institute of Husbandry and Pharmaceutical Sciences, China. The experimental procedure was approved by the institutional ethics committee of the Lanzhou Institute of Husbandry and Pharmaceutical Sciences, China. The ethics certificate number was SCXK (Gan) 2020–0007.

Author contributions

Hongfei Si, Jiao Mo, Siyang Liu, Minghao Cai, Qingyuan Zeng and Zhendi Liu evaluated the *in vitro* and *in vivo* anti-*T. gondii* activity. Jiyu Zhang and Jili Zhang supervised the experiments. Jiao Mo wrote the manuscript. Jingjing Fang revised the manuscript. All authors have read and agreed to the published version of the manuscript.

Declarations of competing interest

The authors declare that this research was conducted in the absence of any commercial or financial relationships that could be construed as a potential conflict of interest. The final article has been approved by all the authors.

Acknowledgments

This research was funded by the National Natural Science Foundation of China/Youth Science Foundation Project, China (82102426); Natural Science Foundation of Zhejiang Province, China (LQ22H190001); State Key Laboratory of Veterinary Etiological Biology Open Fund, China (SKLVEB2021KFKT007) and Natural Science Foundation of Ningbo, China (2021J103).

References

Acharjee, R., Talaam, K.K., Hartuti, E.D., et al., 2021. Biochemical studies of mitochondrial malate: quinone oxidoreductase from Toxoplasma gondii. Int. J. Mol. Sci. 22 (15), 7830.

Bajohr, L.L., Ma, L., Platte, C., et al., 2010. In vitro and in vivo activities of 1-hydroxy-2-alkyl-4(1H) quinolone derivatives against Toxoplasma gondii. Antimicrob. Agents Chemother. 54 (1), 517–521.
Bergin, C., et al., 1992. Toxoplasma pneumonitis: fatal presentation of disseminated toxoplasmosis in a patient with AIDS. Eur. Respir. J. 5 (8), 1018–1020.
Deng, Y., Wu, T., Zhai, S.Q., Li, C.H., 2019. Recent progress on anti-Toxoplasma drugs discovery: design, synthesis and screening. Eur. J. Med. Chem. 183, 111711.
Doggett, J.S., Nilsen, A., Forquer, I., et al., 2012. Endochin-like quinolones are highly efficacious against acute and latent experimental toxoplasmosis. Proc. Natl. Acad. Sci. U. S. A. 109 (39), 15936–15941.
Doggett, J.S., Schultz, T., Miller, A.J., et al., 2020. Orally Bioavailable endochin-Like quinolone carbonate ester prodrug reduces Toxoplasma gondii brain cysts. Antimicrob. Agents Chemother. 64 (9) e00535-20.
Giovati, L., Ciociola, T., Magliani, W., Conti, S., 2018. Antimicrobial peptides with antiprotozoal activity: current state and future perspectives. Future Med. Chem. 10 (22), 2569–2572.
Gómez, E., Marín, J.E., Zuluaga, J.D., Pechené, Campo, E.J., et al., 2018. Polymerase chain reaction (PCR) in ocular and ganglionar toxoplasmosis and the effect of therapeutics for prevention of ocular involvement in South American setting. Acta Trop. 184, 83–87.
Hazan, R., Que, Y.A., Maura, D., et al., 2016. Auto poisoning of the respiratory chain by a quorum-sensing-regulated molecule favors biofilm formation and antibiotic tolerance. Curr. Biol. 26 (2), 195–206.
Hegewald, J., Gross, U., Bohne, W., 2013. Identification of dihydroorotate dehydrogenase as a relevant drug target for 1-hydroxyquinolones in Toxoplasma gondii. Mol. Biochem. Parasitol. 190 (1), 6–15.
Kerscher, S., Dröse, S., Zickermann, V., Brandt, U., 2008. The three families of respiratory NADH dehydrogenases. Results Probl. Cell Differ. 45, 185–222.
Konstantinovic, N., Guegan, H., Stäjner, T., Belaz, S., Robert-Gangneux, F., 2019. Treatment of toxoplasmosis: current options and future perspectives. Food Waterborne Parasitol. 15, e00036.
Lin, S.S., Kerscher, S., Saleh, A., et al., 2008. The Toxoplasma gondii type-II NADH dehydrogenase TgNDH2-I is inhibited by 1-hydroxy-2-alkyl-4(1H) quinolones. Biochim. Biophys. Acta 1777 (11), 1455–1462.
Melo, A.M., Bandeiras, T.M., Teixeira, M., 2004. New insights into type II NAD(P)H: quinone oxidoreductases. Microbiol. Mol. Biol. Rev. 68 (4), 603–616.
Melo, E.J., Attias, M., De Souza, W., 2000. The single mitochondrion of tachyzoites of Toxoplasma gondii. J. Struct. Biol. 130, 27–33.
Mital, J., Ward, G.E., 2008. Current and emerging approaches to studying invasion in apicomplexan parasites. Subcell. Biochem. 47, 1–32.
Musso, L., Fabbrini, A., Dallavalle, S., 2020. Natural compound-derived cytochrome bc1 complex inhibitors as antifungal agents. Molecules 25 (19), 4582.
Petri, J., Shimaki, Y., Jiao, W., et al., 2018. Structure of the NDH-2 - HQNO inhibited complex provides molecular insight into quinone-binding site inhibitors. Biochim. Biophys. Acta, Bioenerg. 1859 (7), 482–490.
Radlinski, L., Rowe, S.E., Kartchner, L.B., et al., 2017. Pseudomonas aeruginosa exoproducts determine antibiotic efficacy against Staphylococcus aureus. PLoS Biol. 15 (11), e2003981.
Robert-Gangneux, F., Dardé, M.L., 2012. Epidemiology of and diagnostic strategies for toxoplasmosis. Clin. Microbiol. Rev. 25 (2), 264–296.
Saleh, A., Friesen, J., Baumeister, S., et al., 2007. Growth inhibition of Toxoplasma gondii and Plasmodium falciparum by nanomolar concentrations of 1-hydroxy-2-dodecyl-4(1H) quinolone, a high-affinity inhibitor of alternative (type II) NADH dehydrogenases. Antimicrob. Agents Chemother. 51 (4), 1217–1222.
Sena, F.V., Batista, A.P., Catarino, T., et al., 2015. Type-II NADH: quinone oxidoreductase from Staphylococcus aureus has two distinct binding sites and is rate limited by quinone reduction. Mol. Microbiol. 98 (2), 272–288.
Sena, F.V., Sousa, F.M., Oliveira, A.S.F., et al., 2018. Regulation of the mechanism of type-II NADH: quinone oxidoreductase from S. aureus. Redox Biol. 16, 209–214.
Sepúlveda-Arias, Juan, C., et al., 2014. Toxoplasmosis as a travel risk. Trav. Med. Infect. Dis. 12, 592–601.
Smith, N.C., Goulart, C., Hayward, J.A., et al., 2021. Control of human toxoplasmosis. Int. J. Parasitol. 51 (2–3), 95–121.
Sul, O.J., Ra, S.W., 2021. Quercetin Prevents LPS-Induced oxidative stress and inflammation by modulating NOX2/ROS/NF-kB in lung epithelial cells. Molecules 26 (22), 6949.
Thierbach, S., Birmes, F.S., Letzel, M.C., et al., 2017. Chemical modification and detoxification of the Pseudomonas aeruginosa Toxin 2-Heptyl-4-hydroxyquinoline N-Oxide by environmental and pathogenic bacteria. ACS Chem. Biol. 12 (9), 2305–2312.
Thierbach, S., Wienhold, M., Fetzner, S., Hennecke, U., 2019. Synthesis and biological activity of methylated derivatives of the Pseudomonas metabolites HHQ, HQNO and PQS. Beilstein J. Org. Chem. 15, 187–193.
Vallières, C., Fisher, N., Antoine, T., et al., 2012. HDQ, a potent inhibitor of Plasmodium falciparum proliferation, binds to the quinone reduction site of the cytochrome bc1 complex. Antimicrob. Agents Chemother. 56 (7), 3739–3747.
Wu, Y., Seyedsayamdost, M.R., 2017. Synergy and target promiscuity drive structural divergence in bacterial alkylquinolone biosynthesis. Cell. Chem. Biol. 24 (12), 1437–1444.
Zhang, J.L., Si, H.F., Shang, X.F., et al., 2019a. New life for an old drug: in vitro and in vivo effects of the anthelmintic drug niclosamide against Toxoplasma gondii RH strain. Int. j. parasito. Drugs Drug Resist. 9, 27–34.
Zhang, J., Si, H., Li, B., et al., 2019b. Myrislignan exhibits activities against Toxoplasma gondii RH strain by triggering mitochondrial dysfunction. Front. Microbiol. 10, 2152.
Zhang, J., Si, H., Lv, K., et al., 2021. Licarin-B exhibits activity against the Toxoplasma gondii RH Strain by damaging mitochondria and activating autophagy. Front. Cell Dev. Biol. 9, 684393.
Zeng, Q.Y., Si, H.F., Lv, K., et al., 2022. Determination and pharmacokinetics study of UK-5099 in mouse plasma by LC–MS/MS. BMC Vet. Res. 18, 145.